The American Journal of Pathology, Vol. 178, No. 6, June 2011

DOI: 10.1016/j.ajpath.2011.02.004

Vascular Biology, Atherosclerosis, and Endothelium Biology

Microcalcifications in Early Intimal Lesions of Atherosclerotic Human Coronary Arteries

Ruben B. Roijers,* Nicola Debernardi,*
Jack P.M. Cleutjens,† Leon J. Schurgers,‡
Peter H.A. Mutsaers,* and Ger J. van der Vusse§

From the Department of Applied Physics, Eindhoven University of Technology, Eindhoven; and the Departments of Pathology,† Biochemistry,‡ and Physiology,§ Cardiovascular Research Institute Maastricht, Maastricht University, Maastricht, the Netherlands*

Although calcium (Ca) precipitation may play a pathogenic role in atherosclerosis, information on temporal patterns of microcalcifications in human coronary arteries, their relation to expression of calcification-regulating proteins, and colocalization with iron (Fe) and zinc (Zn) is scarce. Human coronary arteries were analyzed post mortem with a proton microprobe for element concentrations and stained (immuno)histochemically for morphological and calcification-regulating proteins. Microcalcifications were occasionally observed in preatheroma type I atherosclerotic intimal lesions. Their abundance increased in type II, III, and IV lesions. Moreover, their appearance preceded increased expression of calcification-regulating proteins, such as osteocalcin and bone morphogenetic protein-2. In contrast, their presence coincided with increased expression of uncarboxylated matrix Gla protein (MGP), whereas the content of carboxylated MGP was increased in type III and IV lesions, indicating delayed posttranslational conversion of biologically inactive into active MGP. Ca/phosphorus ratios of the microcalcifications varied from 1.6 to 3.0, including amorphous Ca phosphates. Approximately 75% of microcalcifications colocalized with the accumulation of Fe and Zn. We conclude that Ca microprecipitation occurs in the early stages of atherosclerosis, inferring a pathogenic role in the sequel of events, resulting in overt atherosclerotic lesions. Microcalcifications may be caused by local events triggering the precipitation of Ca rather than by increased expression of calcification-regulating proteins. The high degree of colocalization with Fe and Zn suggests a mutual relationship between these trace elements and early deposition of Ca salts. ***(Am J Pathol 2011, 178:2879–2887; DOI: 10.1016/j.ajpath.2011.02.004)***

According to the current paradigm, atherosclerosis starts with the deposition of lipid material originating from low-density lipoproteins, invasion of macrophages, eventually differentiating into foam cells, proliferation of smooth muscle cells, and enhanced production of extracellular matrix proteins in response to chronic arterial inflammation.[1–3] In addition to biochemical and cellular changes, increased deposition of calcium (Ca)–rich material and trace elements, such as iron (Fe) and zinc (Zn), has been reported.[4–7] In general, vascular calcifications, predominantly in the thickened intima, have been associated with more advanced stages of atherosclerosis.[8–11] Large calcified material at a millimeter scale correlated with plaque burden and predisposition to myocardial infarction.[12,13] In addition to these nodules or sheets of calcified material, the presence of Ca deposits at a (sub)micrometer scale (ie, microcalcifications) in the atherosclerotic lesion has been reported.[5,8] Recent studies[14,15] showed that rupture of vulnerable plaques in thin fibrous caps because of stress-induced debonding appears to occur more readily in human atherosclerotic lesions in the vicinity of microcalcifications. These findings indicate that microdeposits of Ca-rich material may not be innocent bystanders but are most likely playing a pathogenic role in plaque instability. Moreover, experimental studies[16] in apolipoprotein E–deficient mice showed that deposition of insoluble Ca salts at the micrometer scale is an early event in the atherosclerotic aortic wall. However, information about the time of onset of microcalcifications in human coronary arteries is scarce. Because microcalcifications in the vascular wall might play a pivotal role in the chain of events eventually leading to overt atherosclerotic plaques, information on the relation between microscale Ca deposits and the severity of atherosclerotic lesions in human arterial walls is of great importance.

The causes of Ca deposition in atherosclerotic lesions are still incompletely understood. Calcification-regulatory

Supported by grants FOM 00PMT13 from Stichting voor Fundamenteel Onderzoek der Materie (Foundation for Fundamental Research of Materials).

Accepted for publication February 3, 2011.

Address reprint requests to Ger J. van der Vusse, Ph.D., Department of Physiology, Maastricht University, PO Box 616, 6200 MD Maastricht, the Netherlands. E-mail: vandervusse@maastrichtuniversity.nl.

proteins, such as matrix Gla protein (MGP), osteocalcin (OC), and bone morphogenetic protein-2 (BMP-2), may be actively involved in the calcification process of atherosclerotic lesions.[9,17,18] Alternatively, increased nucleation sites, being apoptotic or necrotic cellular remnants[19,20] and/or matricellular lipidic debris,[21,22] may facilitate the precipitation of Ca salts at the (sub)micrometer scale. Moreover, no consensus exists about the chemical form of the Ca-rich mineralized deposits in the vascular wall. Bulk analysis of human aortas with advanced atherosclerotic lesions revealed a Ca/phosphorus (Ca/P) mass ratio (ie, 2.16) similar to that of hydroxyapatite, being the main constituent of bone.[10] This observation is in line with the notion that calcified material in advanced atherosclerotic lesions of the arterial wall resembles bone and cartilage.[3] In contrast, other researchers[11] found lower Ca/P mass ratios in atherosclerotic plaques. Precursors of hydroxyapatite, such as dicalcium phosphate dehydrate, octacalcium phosphate, or magnesium-substituted tricalcium phosphate (Ca/P mass ratio of 1.29, 1.72, and 1.94, respectively), have also been reported.[23] Information on the chemical composition of microcalcifications in preatheroma stages may facilitate understanding of the mechanisms underlying Ca deposition, and crystal growth, during early atherosclerosis.

Previous studies have shown that trace elements, such as Fe and Zn, accumulate in the atherosclerotic lesions of patients[5,6] and experimental animals.[4,7] Pallon and coworkers[5] reported that microcalcifications and hot spots of Fe and Zn might coincide, in particular in areas close to the internal elastic lamina of the vascular layer. Data on Fe and Zn accumulations and their colocalization with microcalcifications in early atherosclerotic stages in humans are scarce, hampering the rating of the pathogenic significance of increased concentrations of trace elements in the onset and progression of atherosclerosis.

To obtain more information on microcalcifications in early stages of atherosclerosis in human coronary arteries, the main aims of this study were to investigate the following: i) the occurrence of microcalcifications in the thickened intima as a function of severity of the atherosclerotic lesion, ii) the potential role of calcification-regulating proteins in the onset of deposition of Ca-rich material, iii) the Ca/P mass ratio of microcalcifications, and iv) the colocalization of trace elements, such as Fe and Zn, if any, with Ca-rich deposits in the early stages of atherosclerosis.

Therefore, 12 tissue samples of coronary arterial walls of six patients, who died from noncardiac causes, were analyzed with a proton microprobe to determine the presence of locally accumulated Ca, P, and trace elements. The severity of the atherosclerotic lesion of the coronary arterial wall was classified according to the American Heart Association[24] on the basis of standard staining procedures.

Materials and Methods

Elemental Analysis

The elemental composition of human coronary arteries was assessed with a 3-MeV proton beam generated by a 3.5-MV accelerator (Singletron[25]; High Voltage Engineering Europe B.V., Amersfoort, the Netherlands) at Eindhoven University of Technology, Maastricht, the Netherlands. Element analyses were performed using proton-induced X-ray emission (PIXE) in combination with backscattering spectroscopy and forward-scattering spectroscopy. The PIXE technique is used to determine the content (g/cm^2) of all minor and trace elements present in the tissue section with atomic numbers higher than 11; backscattering spectroscopy is used to determine the tissue content of the major elements (ie, carbon, oxygen, and nitrogen), and forward-scattering spectroscopy is used to assess the hydrogen content. The combination of the three techniques results in the concentration (μg/g d.wt. of tissue) of the elements of interest, such as P, Ca, Fe, and Zn, present in the sample. Further details of PIXE analysis of vascular tissue were previously published.[26]

Tissue Preparation

Samples (n = 12) of coronary arteries were collected during autopsy from the hearts of six adults (aged 47 to 86 years) who died from noncardiac causes. Autopsy was performed 6 to 9 hours after death (Department of Pathology, Academic Hospital Maastricht, Maastricht). Tissue collection was approved by the Maastricht Pathology Tissue Collection committee. After excision, vascular wall specimens were placed in cryomolds filled with Tissue Tek (Sakura, Zoeterwoude, the Netherlands), frozen in liquid nitrogen, and stored at -80°C. Cryosections (5-μm thick) were cut at −30°C, using precooled Teflon-coated knives, and subsequently collected on predried Pioloform (Agar Scientific LTD, Stansted, UK) films [thickness, 100 ± 10 nm (mean ± SD)] for PIXE analysis. Adjacent sections (5-μm thick) were collected on glass slides and stored at −20°C before staining. H&E staining was performed immediately after sectioning.

Morphological and IHC Staining

Changes in morphological features were evaluated on H&E-stained sections.[27] Standard oil-red-O staining was applied to evaluate lipid accumulation.[27] Immunohistochemistry (IHC) was performed on frozen sections stained with mouse monoclonal antibodies against both uncarboxylated and carboxylated MGP (ucMGP and cMGP, respectively; 1:25; VitaK Company, Maastricht, the Netherlands),[28] BMP-2[29] (1:20; Genetics Institute, Cambridge, MA), human smooth muscle α-actin (clone 1A4; Dako, Glostrup, Denmark), human macrophage antigen CD68[29] (clone KP1, Dako), or rabbit polyclonal antibodies against OC[29] (1:50; Anawa Trading, Wangen, Zürich, Switzerland). Biotinylated sheep anti-mouse IgG (1:250; Amersham, Little Chalfont, Buckinghamshire, UK) or sheep anti-rabbit IgG (1:1000, Dako) was used as the secondary antibody. After incubation with alkaline phosphatase–coupled avidin-biotin complex (Dako), antibodies were visualized with red alkaline substrate kit I (Vector SK-5100; Vector Laboratories, Burlingame, CA), counter-

stained with hematoxylin, and coverslipped with Entellan. Positive staining appeared red. IHC staining was rated from 0.0 to 5.0; faint diffuse intensities, rated as 0.5, were considered a nonspecific background without (patho-)physiolocal significance. To obtain negative controls only, the secondary antibody was applied.

Tissue Lesion Analysis and Classification

Atherosclerotic lesion subtypes were determined in the 12 samples of human coronary artery walls, according to Stary,[24] by an expert in the field. This American Heart Association classification was based on H&E staining, oil-red-O staining for lipid deposition, and IHC staining for macrophages (CD68) and smooth muscle cells (human smooth muscle α-actin). After classification of the lesion, adjacent sections were analyzed with IHC staining of calcification-regulating proteins. In addition, overview yield scans were made with the 3-MeV proton beam (beam size, 3.0×3.0 μm^2) in adjacent sections. When microcalcifications were visible on the yield scans, areas of interest were reanalyzed with a smaller beam size (commonly, 0.9×0.9 μm^2) to investigate the local element concentrations.

Statistical Analysis

Statistical dependences of data (eg, microcalcification versus IHC scores) were assessed with Spearman's rank correlation analysis.

Results

Stage-Related Features of Microcalcifications and Calcification-Regulating Proteins

From the 12 samples of human coronary artery walls of six patients, four were obtained from the left anterior descending artery, four were obtained from the circumflex artery, and four were obtained from the right coronary artery. On the basis of criteria described by Stary,[24] three samples each could be categorized as type I, II, III, and IV lesions.

The upper row of Figure 1 shows examples of H&E staining. Preatheroma type I lesions were characterized by moderate thickening of the intima and intact lamina elastica interna. In general, type II to IV lesions showed more extensive thickening of the intimal layer with non-disrupted lamina elastica interna. Figure 1 also shows IHC staining of calcification-regulating proteins in the thickened intima of type I to IV lesions. Staining of ucMGP was negative in type I lesions and showed increasing intensity in type I to IV lesions (Figure 1). In contrast, staining of cMGP was weak in both type I and II lesions; and staining intensity substantially increased in type IV lesions (Figure 1). The staining intensity of BMP-2 and OC was faint in type I, II, and III lesions and considerably increased in type IV lesions (Figure 1).

In Figure 2, typical examples of Ca overview scans are presented. In all cases, the Ca yield overview scans made with the microprobe failed to reveal the presence of

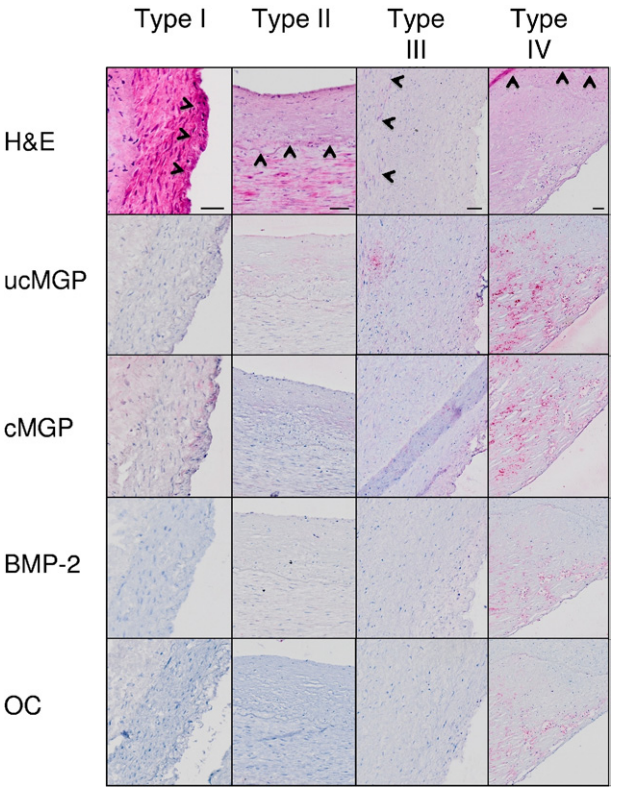

Figure 1. Representative areas of thickened intimal layer of type I, II, III, and IV lesions of human coronary artery wall. Horizontally, the four different classifications are indicated; vertically, the results of H&E and IHC staining of ucMGP, cMGP, BMP-2, and OC are shown. **Arrowheads** indicate the nondisrupted lamina elastica interna in H&E staining of type I, II, III, and IV lesions, separating the intima and media. The IHC signal intensity increases from pale to dark cherry red. Scale bars = 50 μm.

Ca hot spots in the medial and adventitial layers (data not shown). In addition, the Ca yield overview scans of the type I lesions indicated that the thickened intima was almost devoid of Ca hot spots (Figure 2, type I). However, a detailed analysis of the affected intima at a higher magnification with a smaller beam size occasionally revealed the presence of microscale Ca precipitations; the size of the microcalcification generally did not exceed the size of one or two individual pixels (ie, 0.9 μm; Figure 3). Ca yield overview scans clearly showed regions with locally enhanced Ca in the thickened intima of type II lesions (Figure 2, type II). Microcalcifications were also commonly present in the affected intimal layer of type III and IV lesions (Figure 2, types III and IV, respectively).

In Figure 4, the combined results obtained in the 12 coronary artery wall sections under investigation are presented. Nonparametric statistical dependences analysis (Spearman's rank correlation analysis) revealed an excellent correlation between the patterns of microcalcification scores and ucMGP staining (correlation coefficient, 0.933; $P < 0.001$). Microcalcification scores also correlated with staining scores of cMGP, although to a lesser extent than ucMGP (correlation coefficient, 0.672; $P = 0.017$). The less significant correlation between microcalcifications and cMGP staining is most likely caused by the delayed increase of cMGP compared with ucMGP

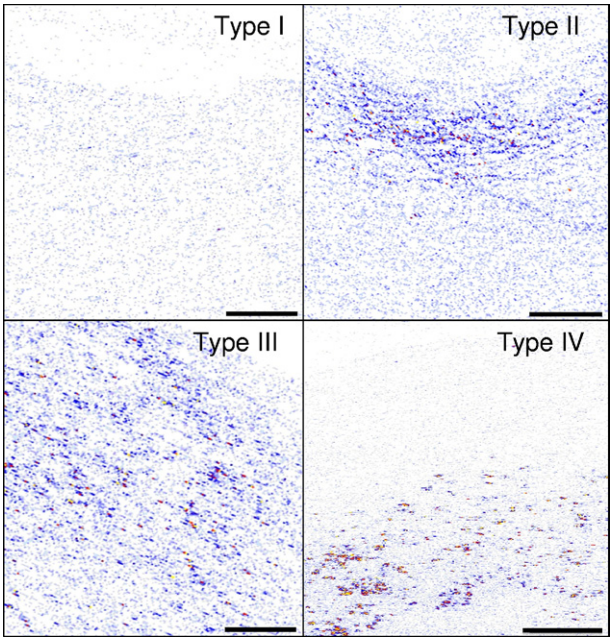

Figure 2. Examples of Ca yield analysis of the thickened intima of type I to IV lesions with the proton microprobe. Microcalcification signal intensity increases from blue to red to yellow. Scale bars = 100 μm.

staining (Figure 4). No significant correlations were found between microcalcification scores and IHC staining of BMP-2 and OC: the occurrence of microcalcifications clearly preceded the increased expression of these calcification-regulating proteins.

Ca/P Mass Ratio

First, areas in intimal type I lesions, which were clearly devoid of Ca hot spots, were used to formulate a criterion to distinguish microcalcifications from surrounding regions. The average intimal Ca concentration in microcalcification-free areas was $4 \pm 2 \times 10^2$ μg/g d.wt., and the

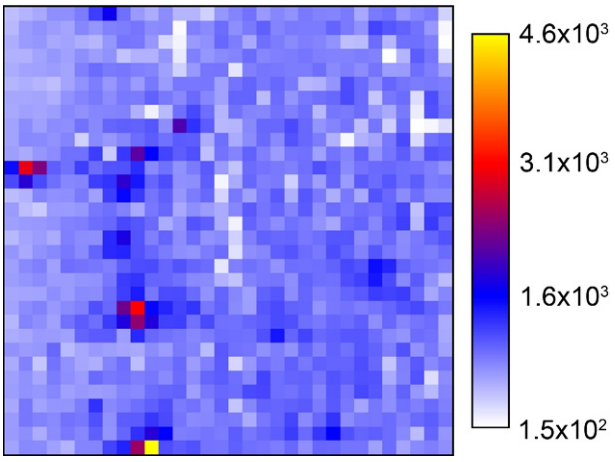

Figure 3. Ca concentration distribution of a randomly chosen area in the thickened intimal layer of a type I lesion. The scan area is 28 μm^2; and pixel size, 0.9 μm. **Right:** Ca concentration is given and expressed as μg/g d.wt. Microcalcification signal intensity increases from blue to red to yellow. The size of the Ca hot spots hardly exceeds one or two pixels.

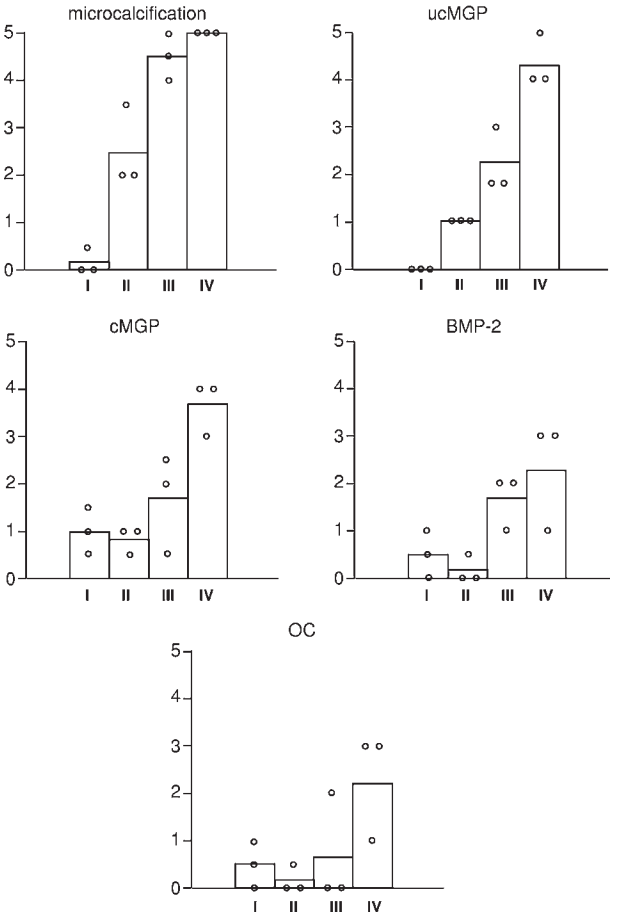

Figure 4. Combined results of Ca yield ("microcalcifications") and immunological staining of ucMGP, cMGP, BMP-2, and OC, assessed in the 12 sections of human coronary artery wall under investigation, are presented. Data were obtained in three lesions each of types I, II, III, and IV. 0 indicates no staining intensity; and 5, highest intensity observed. The height of the bars reflects the mean. An open circle refer to individual values per lesion type.

average Ca/P mass ratio was 0.14 ± 0.09 (mean ± SD). A pixel was categorized as belonging to a microcalcification if the values of Ca concentration and Ca/P mass ratio were larger than defined in the criteria (ie, an average value plus three SDs for both parameters).

To assess the Ca/P mass ratio of microcalcifications in early atherosclerotic lesions, 45 Ca hot spots were randomly selected from sections with type II, III, and IV lesions. First, a region with increased Ca density was chosen on overview scans. Subsequently, areas with one or more Ca hot spots were chosen at random and scanned with a smaller proton beam size (Figure 5A). Thereafter, an area (marked with a square in Figure 5A) was chosen for further magnification with a further reduction in beam size. The results are shown in Figure 5B. Second, a Ca hot spot was randomly chosen to analyze the concentration distribution of Ca and P. Therefore, a high-resolution scan was produced (Figure 5C). The final scans consisted of 32 × 32 pixels, with a scan area of 14 × 14 μm^2. Figure 5 shows excellent colocalization of P and Ca in the microcalcification.

Three representative examples of a Ca/P scatter plot belonging to distinct microcalcifications are shown in

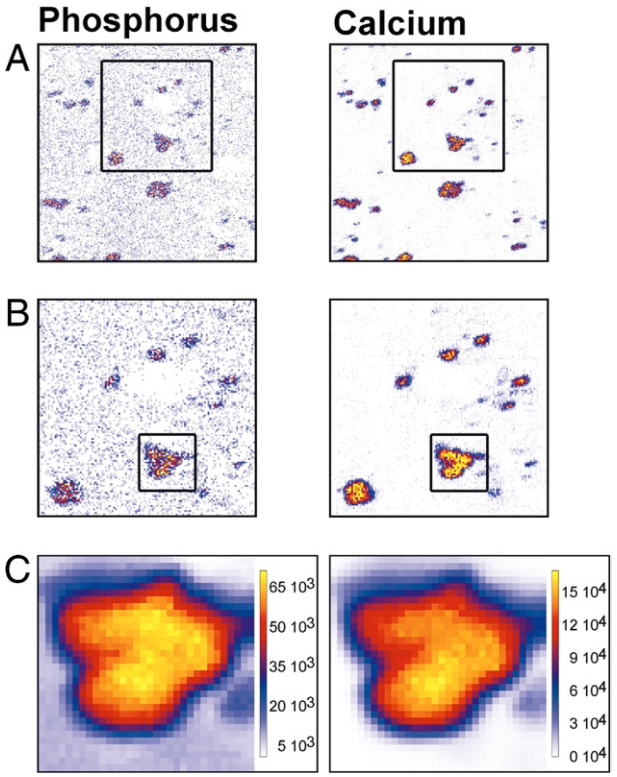

Figure 5. Typical examples of P and Ca yield distributions in the thickened intima of the human coronary artery wall. **A:** A randomly chosen area was analyzed, with a beam size of 0.9 × 0.9 μm^2 and a scan size of 128 × 128 μm^2. The marked area was reanalyzed with a beam size of 0.9 × 0.9 μm^2. **B:** A scan size of 64 × 64 μm^2 is shown. **C:** The concentration distributions of P and Ca of a distinct microcalcification (marked area in **B**). The scan size was 28 × 28 μm^2, and the beam size was 0.9 × 0.8 μm^2. **Right:** Values are expressed as $\mu g/g$ d.wt.

Figure 6A–C. The corresponding scans consisted of 32 × 32 pixels; the quantitative relationship between the mass of Ca and P is shown on the individual pixel base. In these three particular cases, the Ca/P mass ratio was 1.81 ± 0.05 (Figure 6A), 2.10 ± 0.06 (Figure 6B), and 2.79 ± 0.08 (Figure 6C) (mean ± SD).

The small variation (approximately 3%) observed between values of pixels belonging to one individual Ca hot spot strongly suggests a homogeneous Ca and phosphate composition of that particular microcalcification. The same holds for the other 42 Ca microprecipitates analyzed. In contrast to the constant Ca/P mass ratio within each individual Ca hot spot, the ratio appreciably varied between the various Ca precipitates (ie, from approximately 1.6 to 3.0; Figure 6D). This figure, showing the Ca/P mass ratios of 45 microcalcifications in ascending order, clearly indicates a continuum between the lowest and highest mass ratio observed instead of clustering around the ratio of pure hydroxyapatite (ie, 2.16). The median value of the Ca/P mass ratio of the 45 hot spots analyzed was close to 2.1. No relationship was found between severity of lesion and Ca/P mass ratio (data not shown).

Colocalization of Fe and Zn with Microcalcifications

For all 45 Ca hot spots and the immediate surroundings, as previously described, the concentration of the trace elements Fe and Zn was measured with the microprobe technique. The detection limits for Fe and Zn were 7 and 5 $\mu g/g$ d.wt., respectively. Fe and Zn often showed small hot spots, varying in diameter from 1 to 10 μm. For the 45 high-magnification scan areas, colocalization of Fe and Zn with the Ca precipitates was assessed. The criteria were as follows: i) perfect match in localization (Figure 7 provides a typical example), ii) Fe and Zn accumulated in close vicinity to the Ca hot spot (within 2 μm), iii) Fe and Zn locally accumulated in a region more remote from the Ca precipitate (within 2 to 4 μm), or iv) no match at or near the microcalcification. In case of Fe accumulation,

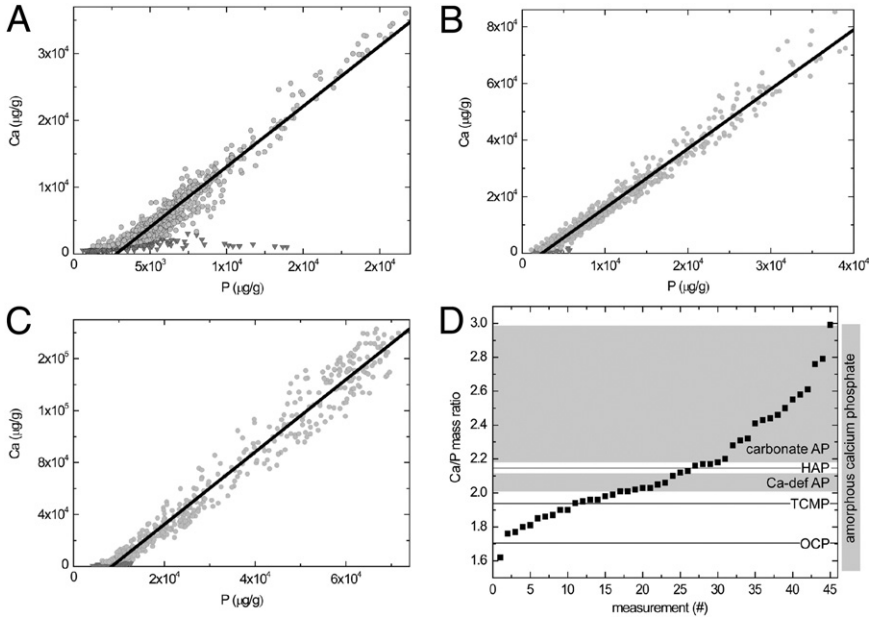

Figure 6. Typical examples of scatter plots of Ca and P concentrations (expressed as $\mu g/g$ d.wt.) in distinct pixels from three individual Ca hot spots (**A–C**). The scan size was 32 × 32 pixels. Light gray circles indicate pixels belonging to the calcification; and dark gray triangles, pixels of the region surrounding the calcification. A linear fit through the points belonging to a distinct microcalcification (light gray circles) is the slope of the line and represents the Ca/P mass ratio (1.81 ± 0.05, 2.10 ± 0.06, and 2.79 ± 0.08 for **A–C**, respectively). **D:** The Ca/P mass ratios of 45 microcalcifications are arranged in ascending order. Different types of Ca phosphate salts are indicated with horizontal lines [octacalcium phosphate (OCP; Ca/P mass ratio, 1.72), magnesium-substituted tricalcium phosphate (TCMP; mass ratio, 1.94), and hydroxyapatite (HAP; mass ratio, 2.16)] or as a gray area [Ca-deficient apatite (Ca-def AP; mass ratio, 2.08 to 2.13) and carbonate apatite (carbonate AP; mass ratio, 2.20 to 2.97)].[23] **Right:** The range of mass ratios of amorphous Ca phosphate is 1.55 to 3.23 (vertical column).

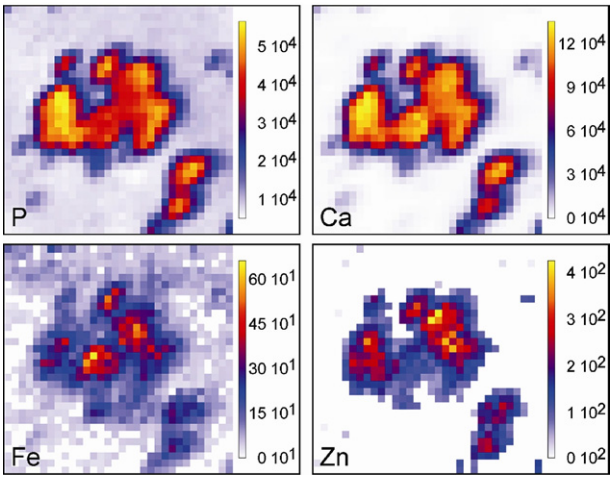

Figure 7. Typical example of concentration distributions of P, Ca, Fe, and Zn in the thickened intima of the human coronary artery (scan size, 14 × 14 μm^2; beam size, 1.0 × 0.9 μm^2). **Right:** Values of element concentrations are expressed as $\mu g/g$ d.wt.

its colocalization with Ca hot spots was perfect in 73% of the cases (Table 1). In 76% of the cases, Zn colocalized perfectly with microcalcifications. In more than two thirds of the cases in which both Fe and Zn accumulated locally, both elements showed excellent spatial correlation (Table 1). No relationship was found between severity of lesion and degree of colocalization of Ca precipitates and Fe and Zn accumulations (data not shown).

Discussion

The deposition of bulk Ca-rich material is generally associated with advanced stages of the atherosclerotic process.[8] A few studies[16,21,22,30] reported the presence of microcalcifications in the atherosclerotic vessel wall in humans. In the present study, microcalcifications were already occasionally observed in the early stage of atherosclerosis (namely, in the moderately thickened intima of preatheroma type I lesions of the human coronary arterial wall). In more advanced lesions (ie, from type II to IV), microcalcifications were commonly observed in the considerably thickened intima. These findings indicate that precipitation of insoluble Ca salts is an early event in the atherosclerotic process.

The primary trigger for Ca precipitation in soft tissues, such as the coronary vascular wall, is still incompletely understood. Ca precipitation could be elicited by an actively regulated process comparable to bone and cartilage mineralization.[3,9,17,18,31,32] Most studies on mechanisms underlying vascular calcification have been performed on advanced atherosclerotic lesions. However, it cannot be excluded that mechanisms underlying the formation of intimal microcalcifications in the earliest atherosclerotic stages are different from the etiology of vascular bone and cartilage formation.[3] Previously, Shanahan and colleagues[32] reported that MGP is expressed by macrophages and smooth muscle cells in advanced atherosclerotic lesions close to precipitated calcified material, possibly to counteract the calcification process. Moreover, MGP expression was increased in cultured vascular cells before deposition of mineralized material, suggesting an up-regulated defense mechanism to prevent calcification.[33] Because Luo and colleagues[34] revealed that the arteries spontaneously calcify in MGP-null mice, the combined findings strongly suggest that MGP prevents mineralization of the vascular wall.

However, MGP is present in at least two forms [ie, the biologically inactive uncarboxylated form and the biologically active carboxylated form (ucMGP and cMGP, respectively)].[35] cMGP is thought to inhibit the formation of Ca salts. Herein, we show that the early deposition of microscale Ca salts coincides with increased expression of biologically inactive ucMGP. Because Ca can induce the expression of MGP,[35–37] the increase in intimal Ca concentration at the microscale is most likely the trigger for increased expression of MGP. Because the initially enhanced MGP concentration (Figure 4) mainly represented the biologically inactive uncarboxylated form, the rate of carboxylation and, therefore, increased concentration of active cMGP clearly does not keep pace with enhanced expression of MGP. The cause of the delayed conversion of ucMGP into cMGP in the early stages of atherosclerosis is incompletely understood; however, it may relate to locally impaired vitamin K metabolism.[35] Retarded posttranslational transformation of ucMGP into cMGP may add to the progression of Ca salt deposition at the microscale in the early stages of coronary artery atherosclerosis because of lack of sufficient activity of calcification-inhibiting proteins.

BMPs are known to stimulate ectopic bone formation.[38] Earlier studies[29,39] showed increased BMP-2 expression in atherosclerotic lesions with enhanced Ca deposition. The corollary of our finding (ie, increased BMP-2 concentration occurred after the earliest signs of Ca deposition) is that BMP-2 is most likely not involved in the onset of Ca precipitation in the early stages of atherosclerosis. In contrast, BMP-2 could play a detrimental role in accelerating the calcification process during later atherosclerotic stages. However, cMGP is able to bind BMP-2 and, therefore, to mitigate its osteogenic activity.[40]

Herein, it is shown that accumulation of OC, a protein able to inhibit bone formation,[41] is a relatively late phenomenon in the atherosclerotic process. Increased OC levels were found only in atheroma type IV lesions, corroborating previous findings[42] in type V and VI lesions in human atherosclerotic carotid arteries. The late expres-

Table 1. Colocalization of Microcalcifications with Fe and/or Zn Deposits

Type of colocalization	Ca-Fe	Ca-Zn	Fe-Zn
i	73	76	69
ii	7	2	7
iii	4	4	4
iv	16	16	20

Data are given as percentages ($n = 45$). Types of colocalization are as follows: i) perfect colocalization, ii) trace element within 2 μm from the microcalcification, iii) trace element within 3 to 4 μm from the microcalcification, and iv) no trace element deposition at or near the microcalcification (ie, within 0 to 4 μm).

sion of OC implies that OC in the affected coronary artery wall may mitigate further Ca precipitation or crystal growth of already formed microcalcifications but fails to prevent the formation of Ca microdeposits at earlier stages of intimal atherosclerosis.

The collective observations suggest that the onset of deposition of Ca-rich material in the atherosclerotic process is caused by local physicochemical events rather than provoked by altered expression of calcification-regulating proteins. Deposition of insoluble Ca salts may start when the solubility product of Ca and anions, such as inorganic phosphate, exceeded locally. However, because most fluid compartments in the human body are supersaturated with respect to Ca and phosphate ions, deposition of Ca-insoluble material is thermodynamically feasible but kinetically hampered under normal physiological circumstances.[43] This implies that, on the one hand, nucleation sites are required for calcification to occur locally and, on the other hand, specific inhibitory factors are present, preventing the unwanted formation of Ca-rich crystalline structures. Disturbed balance between the two processes will result in the deposition of Ca-rich material (eg, in the preatheromatous coronary artery wall). Nucleation sites may be apoptotic and/or necrotic cellular material.[8,20] So-called matrix vesicles or apoptotic bodies provide phospholipids and other lipidic material that could serve as the site for Ca precipitation. Recently, the osteogenic properties of the phospholipid degradation product lysophosphatidylcholine were observed.[44] A close relation between microcalcifications and small pools of extracellular lipids, consisting of cholesterol crystals, was previously observed.[21,22] Moreover, matrical lipidic debris or "matrix vesicles" facilitated the deposition of Ca-rich material.[37,45] The extracellular localization of this type of nidus was groupwise positioned along elastic fibers and smooth muscle cells.[4,11,30,46,47] In contrast, Stary[8] suggested that Ca precipitation starts intracellularly, predominantly in smooth muscle cells, before cell death. Later studies[48] support this notion. The present technique does not allow for discrimination between intracellular and extracellular sites of Ca microdeposits. Further miniaturization of the proton beam to the submicrometer level is required to adequately address this intriguing issue.

Because the Ca/P mass ratio might reveal the nature of the insoluble Ca salt and, therefore, possible similarities between physiological bone formation and pathophysiological mineralization of soft tissues, the Ca/P mass ratio in 45 individual Ca hot spots was assessed. In previous studies, chemical bulk analysis of both large and small calcified deposits in human aortas with advanced atherosclerotic lesions[10] showed Ca/P mass ratios close to that of pure hydroxyapatite (ie, 2.16). Values varying between 2.0 and 2.2 were found in human calcified coronary arteries, investigated with the electron microprobe.[49] Finally, Bobryshev[50] showed a Ca/P mass ratio of 2.12 ± 0.18 of calcified vesicles (size, 0.1 to 0.5 μm) (mean ± SD). In contrast, low ratios (0.66 ± 0.22, mean ± SD) were found in calcified matrix vesicles in human aortic and carotid arteries.[51] Moreover, a value of 1.81 was reported for calcifications in human aortas,[11] suggesting the presence of Ca-deficient hydroxyapatite. The present determination of Ca/P mass ratios of intimal microcalcifications indicated that based on individual pixels individual, Ca hot spots possess their own unique ratio, indicating a homogeneous crystal composition. In contrast, the Ca/P mass ratio greatly varied from precipitate to precipitate, ranging from 1.6 to 3.0, indicating that the composition of Ca- and P-rich material in the early stages of atherosclerosis is not identical to that of hydroxyapatite (Ca/P mass ratio, 2.16), being the main constituent of mature bone.[43] The composition could be amorphous Ca phosphate or combinations thereof, with carbonated Ca phosphate, dicalcium phosphate dehydrate, octacalcium phosphate, and magnesium-substituted tricalcium phosphate. Because the median value of the Ca/P mass ratio of 45 microcalcifications analyzed is close to 2.1, analysis of pooled material, as performed in previous studies,[10] could have easily obscured the true composition of the microscale Ca deposits and could have erroneously led to the conclusion that microcalcifications in soft tissue show a high degree of similarity to mature mineralized bone. However, Raman spectroscopic analysis of early mineralization in bone revealed the presence of highly disordered amorphous Ca phosphate in conjunction with octacalcium phosphate rather than pure hydroxyapatite.[52] Additional analytical techniques, such as electron diffraction, are necessary to reveal the precise chemical composition of the Ca microdeposits in the early atherosclerotic lesions.

Herein, we found that, in the early stages of intimal atherosclerosis, small hot spots of Fe and Zn were already present in approximately 75% of the cases spatially coinciding with microcalcifications. Fe deposits have been observed in advanced atherosclerotic lesions.[6,7,53] Fe was surrounded by Ca-rich material, close to the lamina elastica interna of human coronary arteries.[5] Unfortunately, the severity of the atherosclerotic lesion was not classified. Both increased[5] and decreased[7] Zn concentrations in atherosclerotic tissue have been reported. Fe and Zn in the pathogenesis of atherosclerosis could have multiple roles. Fe could provoke peroxidation of lipids, either engulfed by macrophages or deposited extracellularly.[54,55] Zn is a cofactor of superoxide dismutase, scavenging oxygen-free radicals and, thus, inhibiting lipid peroxidation. Zn is also present in matrix metalloproteases, degrading tissue extracellular matrix and promoting plaque rupture.[56] The present experimental approach does not allow drawing firm conclusions about the source and pathogenic significance of Fe and Zn, but their presence in the early stages of atherosclerosis, commonly in conjunction with increased Ca precipitation, may imply a role in the onset and progression of vascular calcification.

Recent findings[57] showed that exposure of macrophages to Ca microcrystals with a diameter of 1 to 2 μm elicited a proinflammatory response, suggesting that the early occurrence of microcalcifications in the intimal layer may negatively affect the atherosclerotic process by locally stimulating an inflammatory process. Moreover, in the vessel wall of apolipoprotein E2–deficient mice, invasion of proinflammatory macrophages preceded deposi-

tion of Ca crystals.[16] These findings suggest a positive feedback amplification loop of microcalcifications and vascular inflammation. The observation that Ca phosphate crystals with a diameter of approximately 1 μm induced death of vascular smooth muscle cells *in vitro*[58] might indicate a vicious cycle of deposition of microcalcifications, cell death, formation of apoptotic bodies and matrix vesicles, and subsequent precipitation of Ca salts. Whether this devastating process also occurs in human coronary vasculature remains to be determined.

In summary, the deposition of Ca-rich material in the intimal layer of human coronary arteries is an early event in the atherosclerotic process. Precipitation of Ca-rich material at the micrometer scale occurred before changes in the intimal content of calcification-regulating proteins, such as OC and BMP-2, but coincided with enhanced expression of ucMGP. The rate of MGP carboxylation, yielding the biologically active form cMGP, initially did not keep pace with enhanced MGP expression. The Ca/P mass ratio of the microcalcifications corresponds to amorphous Ca phosphate rather than pure hydroxyapatite. In approximately 75% of all the Ca hot spots investigated, Zn and Fe coprecipitated, suggesting a mutual relation between the early precipitation of Ca and accumulation of these two trace elements. Although the present study does not elucidate the precise mechanism underlying the precipitation of Ca-rich material in the human coronary arterial wall, the collective findings might imply that early-stage microcalcifications play a pathological role in the onset and progression of vascular disease.

References

1. Lusis AJ: Atherosclerosis. Nature 2000, 407:233–241
2. Libby P: Current concepts of the pathogenesis of the acute coronary syndromes. Circulation 2001, 104:365–372
3. Mohler ER 3rd: Mechanisms of aortic valve calcification. Am J Cardiol 2004, 94:1396–1402
4. Minqin R, Watt F, Huat BT, Halliwell B: Correlation of iron and zinc levels with lesion depth in newly formed atherosclerotic lesions. Free Radic Biol Med 2003, 34:746–752
5. Pallon J, Homman P, Pinheiro T, Halpern MJ, Malmqvist K: A view on elemental distribution alterations of coronary artery walls in atherogenesis. Nucl Instrum Methods Phys Res B 1995, 104:344–350
6. Lee FY, Lee TS, Pan CC, Huang AL, Chau LY: Colocalization of iron and ceroid in human atherosclerotic lesions. Atherosclerosis 1998, 138:281–288
7. Makjanic J, Ponraj D, Tan BKH, Watt F: Nuclear microscopy investigations into the role of iron in atherosclerosis. Nucl Instrum Methods Phys Res B 1999, 158:356–360
8. Stary HC: Natural history of calcium deposits in atherosclerosis progression and regression. Z Kardiol 2000, 89(Suppl 2):28–35
9. Doherty TM, Fitzpatrick LA, Inoue D, Qiao JH, Fishbein MC, Detrano RC, Shah PK, Rajavashisth TB: Molecular, endocrine, and genetic mechanisms of arterial calcification. Endocr Rev 2004, 25:629–672
10. Schmid K, McSharry WO, Pameijer CH, Binette JP: Chemical and physicochemical studies on the mineral deposits of the human atherosclerotic aorta. Atherosclerosis 1980, 37:199–210
11. Becker A, Epple M, Muller KM, Schmitz I: A comparative study of clinically well-characterized human atherosclerotic plaques with histological, chemical, and ultrastructural methods. J Inorg Biochem 2004, 98:2032–2038
12. Sangiorgi G, Rumberger JA, Severson A, Edwards WD, Gregoire J, Fitzpatrick LA, Schwartz RS: Arterial calcification and not lumen stenosis is highly correlated with atherosclerotic plaque burden in humans: a histologic study of 723 coronary artery segments using nondecalcifying methodology. J Am Coll Cardiol 1998, 31:126–133
13. Beadenkopf WG, Daoud AS, Love BM: Calcification in the coronary arteries and its relationship to arteriosclerosis and myocardial infarction. Am J Roentgenol Radium Ther Nucl Med 1964, 92:865–871
14. Vengrenyuk Y, Carlier S, Xanthos S, Cardoso L, Ganatos P, Virmani R, Einav S, Gilchrist L, Weinbaum S: A hypothesis for vulnerable plaque rupture due to stress-induced debonding around cellular microcalcifications in thin fibrous caps. Proc Natl Acad Sci U S A 2006, 103: 14678–14683
15. Ehara S, Kobayashi Y, Yoshiyama M, Shimada K, Shimada Y, Fukuda D, Nakamura Y, Yamashita H, Yamagishi H, Takeuchi K, Naruko T, Haze K, Becker AE, Yoshikawa J, Ueda M: Spotty calcification typifies the culprit plaque in patients with acute myocardial infarction: an intravascular ultrasound study. Circulation 2004, 110:3424–3429
16. Aikawa E, Nahrendorf M, Figueiredo JL, Swirski FK, Shtatland T, Kohler RH, Jaffer FA, Aikawa M, Weissleder R: Osteogenesis associates with inflammation in early-stage atherosclerosis evaluated by molecular imaging in vivo. Circulation 2007, 116:2841–2850
17. Shanahan CM, Proudfoot D, Tyson KL, Cary NR, Edmonds M, Weissberg PL: Expression of mineralisation-regulating proteins in association with human vascular calcification. Z Kardiol 2000, 89(Suppl 2):63–68
18. Vattikuti R, Towler DA: Osteogenic regulation of vascular calcification: an early perspective. Am J Physiol Endocrinol Metab 2004, 286: E686–E696
19. Stary HC: The development of calcium deposits in atherosclerotic lesions and their persistence after lipid regression. Am J Cardiol 2001, 88:16E–19E
20. Proudfoot D, Skepper JN, Hegyi L, Farzaneh-Far A, Shanahan CM, Weissberg PL: The role of apoptosis in the initiation of vascular calcification. Z Kardiol 2001, 90(Suppl 3):43–46
21. Guyton JR, Klemp KF: Transitional features in human atherosclerosis: intimal thickening, cholesterol clefts, and cell loss in human aortic fatty streaks. Am J Pathol 1993, 143:1444–1457
22. Jeziorska M, McCollum C, Woolley DE: Calcification in atherosclerotic plaque of human carotid arteries: associations with mast cells and macrophages. J Pathol 1998, 185:10–17
23. LeGeros RZ: Formation and transformation of calcium phosphates: relevance to vascular calcification. Z Kardiol 2001, 90(Suppl 3): 116–124
24. Stary HC: Natural history and histological classification of atherosclerotic lesions: an update. Arterioscler Thromb Vasc Biol 2000, 20: 1177–1178
25. Mous DJW, Haitsma RG, Butz T, Flagmeyer RH, Lehmann D, Vogt J: The novel ultrastable HVEE 3.5 MV Singletron accelerator for nanoprobe applications. Nucl Instrum Methods Phys Res B 1997, 130: 31–36
26. Roijers RB, Dutta RK, Cleutjens JP, Mutsaers PH, de Goeij JJ, van der Vusse GJ: Early calcifications in human coronary arteries as determined with a proton microprobe. Anal Chem 2008, 80:55–61
27. Bancroft JD, Cook HC: Manual of Histological Techniques and Their Diagnostic Application. Edinburgh, Churchill Livingstone, 1994
28. Schurgers LJ, Teunissen KJ, Knapen MH, Kwaijtaal M, van Diest R, Appels A, Reutelingsperger CP, Cleutjens JP, Vermeer C: Novel conformation-specific antibodies against matrix gamma-carboxyglutamic acid (Gla) protein: undercarboxylated matrix Gla protein as marker for vascular calcification. Arterioscler Thromb Vasc Biol 2005, 25:1629–1633
29. Dhore CR, Cleutjens JP, Lutgens E, Cleutjens KB, Geusens PP, Kitslaar PJ, Tordoir JH, Spronk HM, Vermeer C, Daemen MJ: Differential expression of bone matrix regulatory proteins in human atherosclerotic plaques. Arterioscler Thromb Vasc Biol 2001, 21:1998–2003
30. Bobryshev YV, Lord RS, Warren BA: Calcified deposit formation in intimal thickenings of the human aorta. Atherosclerosis 1995, 118:9–21
31. Trion A, van der Laarse A: Vascular smooth muscle cells and calcification in atherosclerosis. Am Heart J 2004, 147:808–814
32. Shanahan CM, Cary NR, Metcalfe JC, Weissberg PL: High expression of genes for calcification-regulating proteins in human atherosclerotic plaques. J Clin Invest 1994, 93:2393–2402
33. Canfield AE, Doherty MJ, Kelly V, Newman B, Farrington C, Grant ME, Boot-Handford RP: Matrix Gla protein is differentially expressed during the deposition of a calcified matrix by vascular pericytes. FEBS Lett 2000, 487:267–271

34. Luo G, Ducy P, McKee MD, Pinero GJ, Loyer E, Behringer RR, Karsenty G: Spontaneous calcification of arteries and cartilage in mice lacking matrix GLA protein. Nature 1997, 386:78–81
35. Schurgers LJ, Cranenburg EC, Vermeer C: Matrix Gla-protein: the calcification inhibitor in need of vitamin K. Thromb Haemost 2008, 100:593–603
36. Proudfoot D, Skepper JN, Shanahan CM, Weissberg PL: Calcification of human vascular cells in vitro is correlated with high levels of matrix Gla protein and low levels of osteopontin expression. Arterioscler Thromb Vasc Biol 1998, 18:379–388
37. Reynolds JL, Joannides AJ, Skepper JN, McNair R, Schurgers LJ, Proudfoot D, Jahnen-Dechent W, Weissberg PL, Shanahan CM: Human vascular smooth muscle cells undergo vesicle-mediated calcification in response to changes in extracellular calcium and phosphate concentrations: a potential mechanism for accelerated vascular calcification in ESRD. J Am Soc Nephrol 2004, 15:2857–2867
38. Hruska KA, Mathew S, Saab G: Bone morphogenetic proteins in vascular calcification. Circ Res 2005, 97:105–114
39. Bostrom K, Watson KE, Horn S, Wortham C, Herman IM, Demer LL: Bone morphogenetic protein expression in human atherosclerotic lesions. J Clin Invest 1993, 91:1800–1809
40. Wallin R, Cain D, Hutson SM, Sane DC, Loeser R: Modulation of the binding of matrix Gla protein (MGP) to bone morphogenetic protein-2 (BMP-2). Thromb Haemost 2000, 84:1039–1044
41. Ducy P, Desbois C, Boyce B, Pinero G, Story B, Dunstan C, Smith E, Bonadio J, Goldstein S, Gundberg C, Bradley A, Karsenty G: Increased bone formation in osteocalcin-deficient mice. Nature 1996, 382:448–452
42. Bini A, Mann KG, Kudryk BJ, Schoen FJ: Noncollagenous bone matrix proteins, calcification, and thrombosis in carotid artery atherosclerosis. Arterioscler Thromb Vasc Biol 1999, 19:1852–1861
43. Dorozhkin SV, Epple M: Biological and medical significance of calcium phosphates. Angew Chem Int Ed Engl 2002, 41:3130–3146
44. Vickers KC, Castro-Chavez F, Morrisett JD. Lyso-phosphatidylcholine induces osteogenic gene expression and phenotype in vascular smooth muscle cells. Atherosclerosis 2010, 211:122–129
45. Ghadially FN: As you like it, part 3: a critique and historical review of calcification as seen with the electron microscope. Ultrastruct Pathol 2001, 25:243–267
46. Kockx MM: Apoptosis in the atherosclerotic plaque: quantitative and qualitative aspects. Arterioscler Thromb Vasc Biol 1998, 18:1519–1522
47. Bobryshev YV: Calcification of elastic fibers in human atherosclerotic plaque. Atherosclerosis 2005, 180:293–303
48. Azari F, Vali H, Guerquin-Kern JL, Wu TD, Croisy A, Sears SK, Tabrizian M, McKee MD: Intracellular precipitation of hydroxyapatite mineral and implications for pathologic calcification. J Struct Biol 2008, 162:468–479
49. Fitzpatrick LA, Severson A, Edwards WD, Ingram RT: Diffuse calcification in human coronary arteries: association of osteopontin with atherosclerosis. J Clin Invest 1994, 94:1597–1604
50. Bobryshev YV: Transdifferentiation of smooth muscle cells into chondrocytes in atherosclerotic arteries in situ: implications for diffuse intimal calcification. J Pathol 2005, 205:641–650
51. McCormick MM, Rahimi F, Bobryshev YV, Gaus K, Zreiqat H, Cai H, Lord RS, Geczy CL: S100A8 and S100A9 in human arterial wall: implications for atherogenesis. J Biol Chem 2005, 280:41521–41529
52. Crane NJ, Popescu V, Morris MD, Steenhuis P, Ignelzi MA Jr: Raman spectroscopic evidence for octacalcium phosphate and other transient mineral species deposited during intramembranous mineralization. Bone 2006, 39:434–442
53. Stadler N, Lindner RA, Davies MJ: Direct detection and quantification of transition metal ions in human atherosclerotic plaques: evidence for the presence of elevated levels of iron and copper. Arterioscler Thromb Vasc Biol 2004, 24:949–954
54. Gaut JP, Heinecke JW: Mechanisms for oxidizing low-density lipoprotein: insights from patterns of oxidation products in the artery wall and from mouse models of atherosclerosis. Trends Cardiovasc Med 2001, 11:103–112
55. Stocker R, Keaney JF Jr: Role of oxidative modifications in atherosclerosis. Physiol Rev 2004, 84:1381–1478
56. Heinecke JW: Oxidative stress: new approaches to diagnosis and prognosis in atherosclerosis. Am J Cardiol 2003, 91:12A–16A
57. Nadra I, Boccaccini AR, Philippidis P, Whelan LC, McCarthy GM, Haskard DO, Landis RC: Effect of particle size on hydroxyapatite crystal-induced tumor necrosis factor alpha secretion by macrophages. Atherosclerosis 2008, 196:98–105
58. Ewence AE, Bootman M, Roderick HL, Skepper JN, McCarthy G, Epple M, Neumann M, Shanahan CM, Proudfoot D: Calcium phosphate crystals induce cell death in human vascular smooth muscle cells: a potential mechanism in atherosclerotic plaque destabilization. Circ Res 2008, 103:e28–e34